Transactions of the **14th International Conference on Structural Mechanics in Reactor Technology** (SMiRT 14), Lyon, France, August 17-22, 1997 **JSP/6**

A review of rheological concrete models for aircraft impact problems in nuclear power plant

de Gayffier A.[(1)], **Duval C.**[(2)]
(1) CEA, France
(2) EDF, France

Abstract

In this paper we describe the use of non linear rheological models for concrete in the computation of vibration in a nuclear power plant induced by an airplane crash. Three different models were reviewed and comparative computations are presented to assess the suitability of those models as far as energy spreading is concerned.

1 INTRODUCTION

The design of nuclear power plant components requires sometimes to withstand military airplane crash. In order to avoid excessive conservatism as well as to take advantage of the increasing capability of computers, 3D Finite-Element models can be used to simulate the subsequent shaking of the structure. With such modelling it is possible to follow the energy as it spreads. An important aspect of such computations is the non-linear behavior of concrete and steel reinforcements, in the vincinity of the impacted zone. So far, considering a modified equivalent loading has obviated the need for non-linear model of concrete and steel [1].

Two main consequences of non-linear behaviour can be brought to light [5]. The first one is the loss of stiffness which inevitably induces extra energy to be transmitted to the structure by the impact force. The second one is the loss of mechanical energy by dissipation (plastic deformation of steel or cracking of concrete). From a dynamic point of view this loss of energy can be regarded as damping. Considering the actual computer capabilities, it is possible to model the non-linear behavior of concrete and steel by appropriate rheological models.

The non-linear models we intend to use must be able to correctly represent the two aspects : loss of stiffness and energy dissipation. Plastic models with hardening are with no doubt adequate to represent the steel reinforcement. However the rheological model currently used for concrete must be reviewed to analyse whether or not they are suitable for our computations. In fact, energy dissipation does not only occur during the impact, but all along the period of shaking. In other words concrete is subjected to cyclic deformation. This particular point will be emphasized in our review of concrete rheological models. We shall consider the relative simplicity of each model as they are intended to be used in an industrial context. We have restricted ourselves to models that are currently available in large scale Finite Element codes namely Plexus and Castem2000 developed by the CEA.

Two plasticity-based models will be described in part 2. In addition we will display the results of computations in which the result of an elastic analysis is compared with a non-linear

one involving one of the two plasticity-based model. The results display a major drawback of the plasticity-based models. In part three a smeared crack-based model is presented along with a similar computation from the second part.

2 PLASTICITY-BASED MODELS

2.1 *The Drucker Prager model*

The Drucker Prager model was one of the first model used to represent concrete [4]. It is implemented under various forms in most of the large scale Finite-Element codes. Its phenomenological basis is the Mohr Coulomb criteria which express the limit on tangential stress relatively to a direction $\vec{n}$ in terms of cohesion and normal stress.

$$\sigma_t \leq c - \tan\phi \,.\, \sigma_n \quad \text{where} \quad \sigma_n = \vec{n} \,.\, \sigma\, \vec{n} \quad \text{and} \quad \sigma_t = \sigma\, \vec{n} - \sigma_n\, \vec{n} \tag{1}$$

The model is formulated in the framework of plasticity. The yield surface is inspired by the previous equation. The following equations summarize the model.

$$\text{The deformation is split into an elastic and a plastic part} \quad \epsilon = \epsilon^{el} + \epsilon^{pl} \tag{2}$$

$$\text{The stress is given by the isotropic Hook law} \quad \sigma = \lambda\, tr\left(\epsilon^{el}\right) Id + 2\mu\, \epsilon^{el} \tag{3}$$

$$\text{The yield criteria is} \quad f = \sigma_{eq} + \alpha P - C \leq 0 \tag{4}$$

$$\text{The plastic flow is given by} \quad \dot{\epsilon}^{pl} = \lambda \times \frac{\partial f}{\partial \sigma} \quad , \quad \lambda \geq 0 \quad \text{and} \quad \lambda \,.\, f = 0 \tag{5}$$

The cohesion C may depend on the cumulated plastic strain p . Considering concrete cracking under uniaxial tension, C should be a decreasing function of p in order to correctly represent the softening induced by tensile crack development in concrete. The two parameters α and C are easily identified by considering unidirectional tensile and compressive test. If σ_T is the maximum admissible stress in tension and $-\sigma_C$ the minimum admissible stress in compression we have the relationships

$$\alpha = 3 \times \frac{\sigma_C - \sigma_T}{\sigma_C + \sigma_T} \qquad C = 2 \times \frac{\sigma_C \times \sigma_T}{\sigma_C + \sigma_T} \tag{6}$$

If one wants to introduce a variation of C, the slopes of the decreasing part of the uniaxial tests must be considered.

Surely the strong points of the Drucker Prager model are simplicity and robustness. However simplicity has a counterpart: the damage induced by tensile crack is crudely represented. In fact the angular point of the yield surface located at $\sigma_{eq} = 0$, $P = \frac{C}{\alpha}$ will "attracts" any state of tension $P > 0$ as C decreases. Eventually tensile cracking drives the stress tensor to an hydrostatic form. Therefore the direction along which the concrete has failed is lost. For any subsequent tension load in other directions, the loss of ultimate strength will occur regardless of the initial direction of load. Such a behaviour is indeed very conservative and not suitable for our gist.

2.2 *Improved plastic models*

In order to overcome these drawbacks, some models have been developped at the CEA in the late 80's. The idea was to remain in the framework of plasticity and to refine the yield surface by

added criteria. For instance the elastic domain was closed in the direction of high compressive stresses ($P < 0$) and criteria involving the principal values of the stress tensor were given which introduced subsequently the directions of possible tensile cracking. The Drucker Prager model was kept to model the damage induced by shear (i.e. high value of σ_{eq}). The work of G. Nahas lead to an improved model [6] which was implemented in Plexus, the CEA fast dynamic code, and Castem2000, the Finite Element code for implicit computations in structural mechanics. We now recall the main points of this model, before we describe its use in an impact-shaking computation. The elastic domain is defined by 6 criteria which correspond to four different modes of concrete degradation. The first one is the damage cause by hydrostatic compression. The criteria is

$$f_1 = -tr(\sigma) - (P_0 + h_1 p_1) \leq 0 \qquad h_1 > 0 \tag{7}$$

where p_1 is the cumulated plastic strain for the induced plastic flow and $h_1 > 0$ is the hardening parameter. The second and third mode of degradation are caused by shear. Ductile and fragile type of behaviour are distinguished depending on the confinement (i.e. the pressure). If $tr(\sigma) < -P_c$ a Von Mises criteria is used for the ductile behavior

$$f_2(\sigma) = \sigma_{eq} - (R_2 + h_2 p_2) \leq 0 \text{ where } h_2 > 0 \tag{8}$$

Now if $tr(\sigma) \geq -P_c$ a Drucker Prager criteria is used for the fragile behavior

$$f_3(\sigma) = \sigma_{eq} + \alpha_3 P - (R_3 + h_3 p_3) \leq 0 \text{ where } h_3 < 0 \tag{9}$$

the sign of h_3 correspond to softening.

The last mode of failure correspond to the generation of macroscopic cracks and is the dominant mode of degradation in our simulation. If σ_1, σ_2 and σ_3 are the eigen values of the stress tensor, along with $\vec{n}_i$ the eigen directions the criteria are

$$f_4^i(\sigma) = \sigma_i - R_4^i \leq 0 \quad i \in \{1, 2, 3\} \tag{10}$$

In all cases the plastic flow is associated. R_i decreases rapidly with the cumulated plastic strain. Once a criteria is meet, $\vec{n}_i$ will remain the direction to express the criteria for the subsequent loads. Therefore one can consider that a macroscopic crack has appeared in the plane perpendicular to $\vec{n}_i$. Although many parameters appear in the model, only a few of them are mandatory. The other ones are computed according to simple functions of the previous one. With respect to our simulation, the major drawback of this model is crack closing. Crack directions have been obtained by the mean of principal directions but the model remain a plastic model and unloading leads inevitably to a linear elastic behaviour. In others words :

$$\text{if} \quad \frac{\partial f}{\partial \sigma} : \dot{\sigma} < 0 \quad \text{then } \dot{\sigma} = \lambda \, tr(\dot{\epsilon}) \, Id + 2\mu\dot{\epsilon} \tag{11}$$

The stiffness recovery is immediate not allowing for a recovery proportional to the closing. Since the model was mainly used for monotonic loading, this was not a major concern. Now in the computation of impact and the subsequent shaking, it is necessary to evaluate the influence of this matter.

2.3 *Illustrative computation : a slab subjected to an impact.*

We consider a cylindrical reinforced concrete slab of radius 20m and thickness 2m. Two horizontal layers of steel bars reinforce the slab, one on each side. Some concentric cylindrical layers spaced every two meters of radius are also used. Concrete is modelled with massive elements

and is characterised by the following parameters $E = 40.GPa$, $\nu = 0.2$, $\rho = 2400\,kg.m^{-3}$, $\sigma_T = 4.MPa$ and $\sigma_C = 40MPa$. Steel reinforcement is modeled with shell elements of thickness $12\,10^{-3}m$. A Von Mises perfectly plastic model is used for steel along with the following characteristics $E = 210.GPa$, $\nu = 0.3$, $\rho = 7800\,kg.m^{-3}$ and $\sigma_{Yield} = 400MPa$. Given the axial symmetry, we used an axisymmetric finite element model with 117 4-node and 3-node massive elements for concrete and 90 2-nodes shell elements. The mesh and the boundary conditions are displayed on figure 1.(a). We used the newly implemented explicit algorithm of Castem2000.

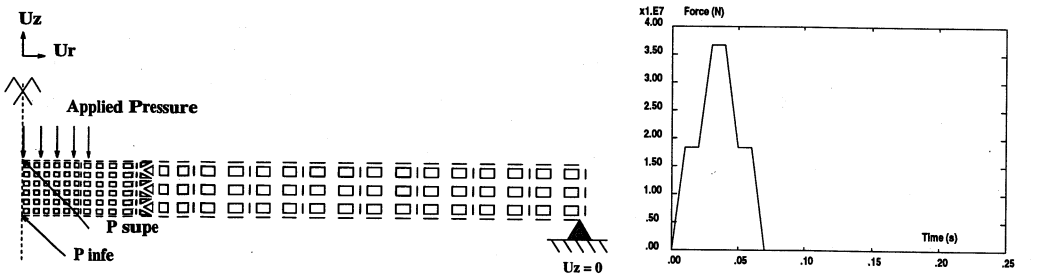

(a) *Mesh* (b) *Impact force evolution*

Figure 1: *Finite element model of the impact.*

The impact is simulated by a uniform pressure applied on the center on a circle of radius one meter. The resulting force evolution is given on figure 1.(b). The time step was $1.7\,10^{-5}s$ and it took 14700 steps to simulate the motion up to $250\,ms$. The vertical displacement of point Pinfe and Psupe are plotted on figure 2 as well as the radial strain ϵ_{rr} at those two locations. For the sake of analysis, the results of a similar computation, in which all materials are elastic are also plotted in dashed lines in both figures 2 and 4.

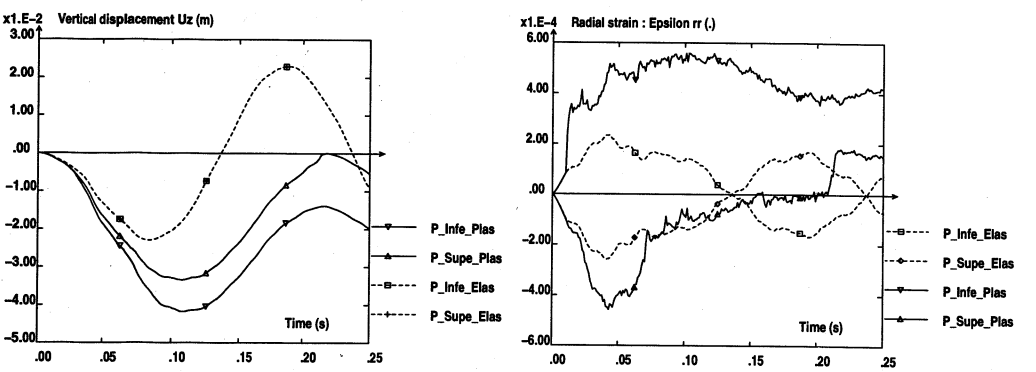

(a) $U_z(t)$ (b) $\epsilon_{rr}(t)$

Figure 2: *Displacement and strain evolution at points Pinfe and Psupe.*

First of all we must remark that the maximal vertical displacement is two times greater

with the plastic model than with the purely elastic model. This is due to the loss of stiffness induced by plastic flow in steel and concrete. Then we should see that displacement is different on each side for the Nahas model. At maximum deflection of the second half period, the end of the bottom side is lower than initially. This effect is essentially the consequence of the way crack close in the Nahas model. Looking at ϵ_{rr} drives to the same conclusion. This component of the strain tensor will remain positive on both sides after cracking occured. The sketch of figure 3 summarize the different stages of this phenomenon.

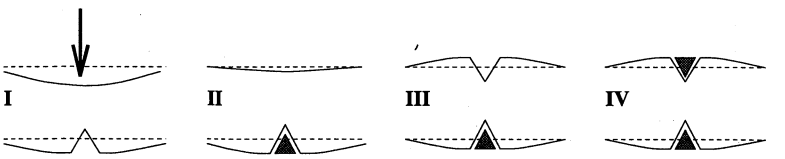

Figure 3: *Interpretation of the residual strain genesis.*

The energy balance is displayed on figure 4. We computed the external energy using the following equations :

$$E_{external}(t) = \int_0^t \int_\Omega F_{ext}(M,s) \,.\, \dot{u}(M,s)\, d\Omega\, ds \qquad E_{kinetic}(t) = \int_\Omega \rho \dot{u}^2(M,t)\, d\Omega$$
$$E_{potential}(t) = \int_\Omega \frac{1}{2}\sigma(M,t) : \epsilon^{el}(M,t)\, d\Omega \qquad E_{dis.}(t) = E_{ext.}(t) - E_{kin.}(t) - E_{pot.}(t) \tag{12}$$

Such a balance is useful to determine the proportion of potential energy "trapped" around the cracks. In order to understand that potential energy is trapped, one can imagine the slab once the motion has damped out. The remaining plastic strain will generate residual stress that correspond to a certain amount of potential energy. Figure 4 shows that potential energy in the plastic computation never decreases to 0 as in the elastic computation. Its level remains above 40 % of the energy provided by the external force. The more potential energy the less kinematics energy. The kinetic energy is also reduced by plastic dissipation. It is interesting to observe that 40% of energy is dissipated after 250 ms. A simple balance indicates that kinetic energy has dropped to 20% of the external energy after the same duration. When we compare it to the elastic kinetic energy, the latter is five times greater even so 20% less energy was provided by the external force in the elastic case.

As a conclusion one must say that the effect of immediate stiffness recovery in cracks closing in the Nahas model is far from negligible. As a rule of thumb it more or less doubles the effect of dissipation on kinetic energy reduction.

3 FICTITIOUS CRACK APPROACH

3.1 *The Dalhbom-Ottosen model*

Smeared cracking is an interesting alternative to plasticity in the representation of tensile cracking in concrete. Dalhbom and Ottosen [2] have proposed a model based on the framework of this approach [3]. The strain rate is the sum of different contributions.

$$\dot{\epsilon} = \dot{\epsilon}^{elas} + \sum_i \dot{\epsilon}_i^f + (\dot{\epsilon}^{th} + \dot{\epsilon}^{pl} + ...) \tag{13}$$

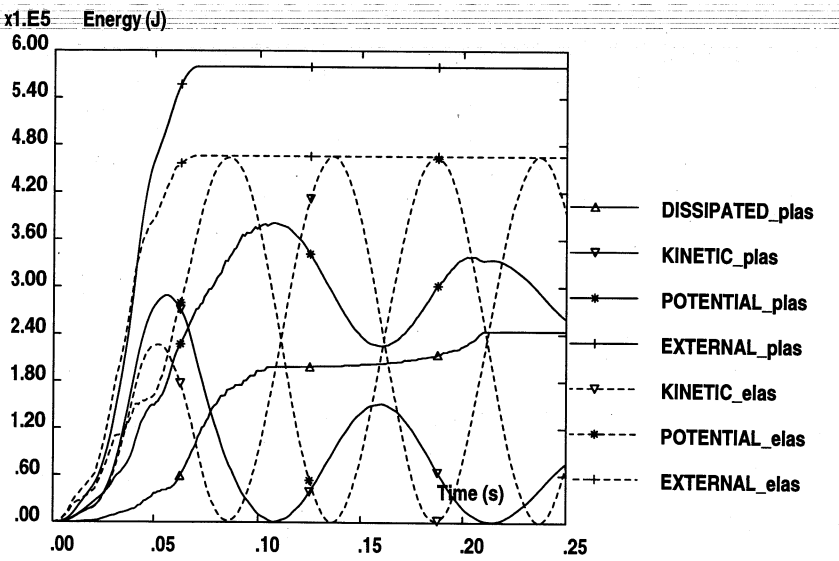

Figure 4: *Energy balance during the simulation*

The term $\dot{\epsilon}_i^f$ represent the kinematic of single crack. If $\vec{n}$ is the direction orthogonal to the crack plane, $\dot{\epsilon}_i^f$ is decomposed into normal strain rate $\vec{n}.\dot{\epsilon}_i^f\,\vec{n}$ and the shear strain $\vec{n}.\dot{\epsilon}_i^f\,\vec{t}$ where $\vec{t}$ si any vector orthogonal to $\vec{n}$. The physical basis of the model is not only the elastic law which relates $\dot{\epsilon}^{elas}$ with $\dot{\sigma}$ but also the relation between $\dot{\epsilon}_i^f$ and $\dot{\sigma}$. Now the behaviour of a macroscopic crack can only be expressed in terms of $\dot{\sigma}$ and $\dot{\vec{w}}$, the relative velocity of its lips. Dalhbom and Ottosen introduce $\vec{w}$ at each sample point by the mean of an equivalent length L, which varies with $\vec{n}$ and the sample point weight. We have

$$\vec{n}.\dot{\epsilon}_i^f\,\vec{n} = \frac{\dot{\vec{w}}.\vec{n}}{L(\vec{n}, M_i)} \tag{14}$$

A complete description of the model is beyond the scope of this paper. There are three important points. First this model is capable of representing the progressive recovery of the stiffness during the crack closing. Second, given a macroscopic crack the energy dissipated during its opening does not depend on the mesh. Of course the number of cracks resulting from loading the structure may depend on the mesh. Last but not least, the model requires only two elastic constants and five other parameters.

3.2 *Illustrative computation*

In order to assess this model in the context of plane crash and subsequent shaking, we performed a similar simulation from section 2. Applied load, boundary conditions and mesh are the same. The model used for steel is also identical. We used the following constants to represent concrete behavior $E = 40.GPa$, $\nu = 0.2$, $\rho = 2400\,kg.m^{-3}$ $\sigma_T = 4.MPa$, $G_s = 5.9MPa$, $G_f = 100.J.m^{-2}$, $\epsilon_{tr} = 3.10^{-3}$

As in section 2, we have plotted the results of the simulation along with the results of a purely elastic computation. Figure 5 displays vertical displacements (a) and radial strain (b)

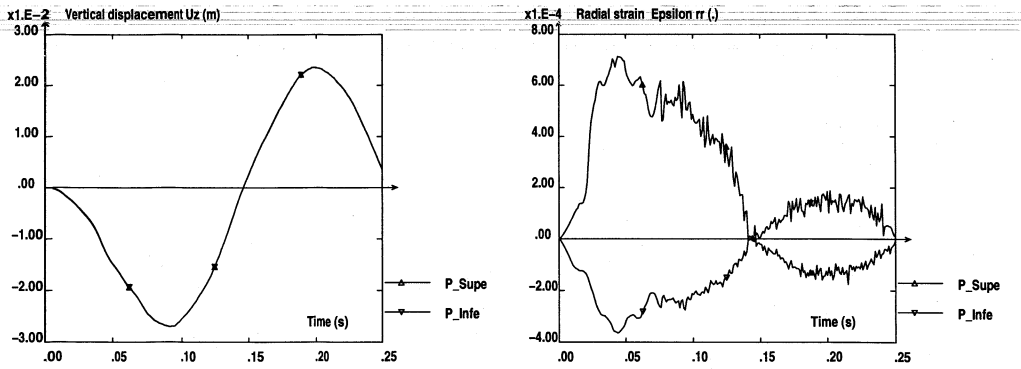

(a) $U_z(t)$ (b) $\epsilon_{rr}(t)$

Figure 5: *Displacement and strain evolution at points Pinf and Psup*

at point Pinfe and Psupe. The vertical displacements are identical on both sides like in the elastic case. They are of course greater than in this latter case. The evolutions of the strain component ϵ_{rr} at Pinfe and Psupe confirm that the cracks closing is adequately represented. Both curves oscillate around their null mean value. The phase decay with regards to the elastic solution is obvious. It is a consequence of the loss of stiffness. In the elastic computation the vertical displacement is harmonic and its frequency is equal to the first eigen frequency of the slab : $4,95\,Hz$. Considering the non-linear computation, we can measure a frequency of $4,77\,Hz$. It corresponds to a 10% loss of stiffness.

In figure 6 we see that the potential energy oscillates during the simulation. But this time its lowest value represents only a few percent of the external energy. Contrary to the previous simulation the decrease of amplitude of motion (kinetic energy) is only due to energy dissipation, which represent 30% of the total energy provided by the impact force after 250 ms.

Additionally we mention that Dalhbom-Ottosen model seems to be stiffer than Nahas model with similar data : the external energy received is 10% less.

4 CONCLUSION

Three different rheological models used for concrete have been reviewed. In the context of plane crash and subsequent shaking, it was shown on a simple computation that the plasticity-based models are not suitable. The immediate stiffness recovery during the crack closing leads to significant residual stress and under estimates the kinetic energy of the structure. The model proposed by Dalhbom and Ottosen was tested on a similar computation and gave satisfactory results.

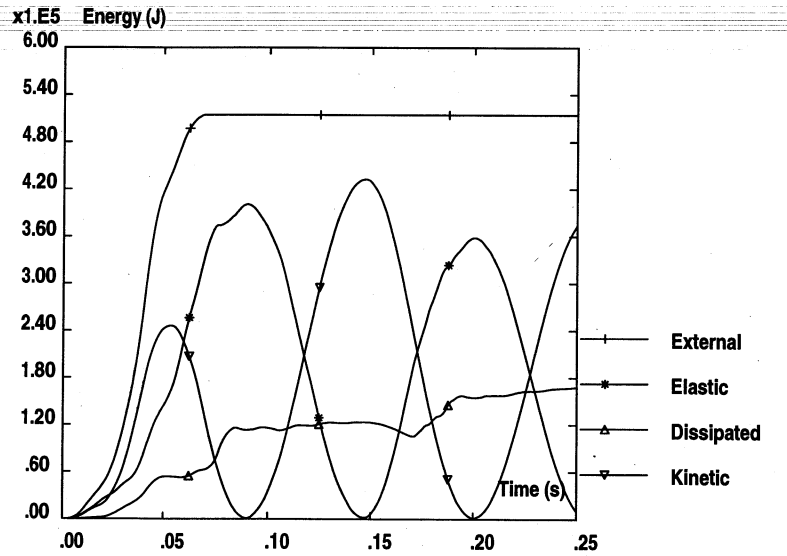

Figure 6: *Energy balance during the simulation*

References

[1] Chadmail, J. F., Krutzik, N. K., and Dubois, T. 1985. Equivalent loading due to airplane impact taking into account the non-linearities of impacted reinforced concrete buildings. *Nuclear Engineering and Design*, 85: 47–57.

[2] Dahlbom, O. and Ottosen, N. S. 1990. Smeared crack analysis using fictitious crck model. *Journal of Engineering mechanics*, 16(1):55–76.

[3] De Borst, R. (1987). Smeared cracking, plasticity creep and thermal loading - Unified approach. *Computer Methods in Applied Mechanics and Engineering*, 62:89–110.

[4] Drucker, D. C. and Prager, W. 1952. Soil mechanics and plastic analysis or limit design. *Quarterly of Applied Mathematics*, 10:157–175.

[5] Duval, C. and Viallet, E. 1996. Vibrations sous séisme et chute d'avion dans les projets nucléaires. *Proc. 4 ieme colloque national AFPS. St Remy les Chevreuse, France.*

[6] Nahas, G. 1986. *Calcul à la ruine des structure en béton.* Thèse de Doctorat, Université Paris VI.